Paper No.
13491

NACE INTERNATIONAL CORROSION Conference & Expo 2019

Phosphate Esters Inhibitors in Naphthenic Acid Corrosion – An Experimental Evaluation

Gheorghe Bota, Peng Jin, Fernando Farelas, Winston Robbins
Ohio University
Institute for Corrosion and Multiphase Technology
342 West State St.
Athens, OH 45701
USA

ABSTRACT

Crude oils with a total acid number (TAN) higher than 0.5 are highly corrosive at temperatures between 400 and 700°F found in atmospheric and vacuum distillations of oil refineries. The destructive effects of naphthenic acids (NAP) occur in the same temperature range as sulfidation corrosion due to reactive sulfur compounds also contained in crude oils. Efforts of mitigating NAP corrosion of existing equipment by a high TAN oil include blending with crudes of lower acids content, neutralization or removal of naphthenic acids, and the use of corrosion inhibitors. Phosphate esters are commonly used in commercial NAP corrosion inhibitors. Two such inhibitors have been evaluated in laboratory experiments using a specific testing – "pretreatment - challenge" procedure. This method evaluates the effects of NAP in oils at high temperature on the formation and corrosion resistance of scales on metal surfaces. NAP corrosivity is determined by weight loss and scales are characterized in cross section by both scanning electron microscopy (SEM) and transmission electron microscopy (TEM) coupled with energy dispersive spectroscopy (EDS). Adding each inhibitor to two crude fractions changed the protective properties of scales formed in the test. The results differentiate the two inhibitors in terms of efficiency and phosphorous distribution in the scale.

Keywords: phosphate esters, corrosion, inhibitors, naphthenic acids, high temperature

INTRODUCTION

Naphthenic acid (NAP) corrosion is an important factor for both refinery operators and design engineers needing to processing crude oils with a TAN higher than 0.5.[1,2] The risk of NAP

corrosion is highest at temperatures 220 - 400°C (430 - 750°F) in atmospheric and vacuum distilling units and is especially high where fluid streams have high velocities or turbulence (transfer lines, pump-arounds, etc) that enhance the acid corrosive effects. Refineries use different strategies to mitigate NAP corrosion, for example, blending the high TAN crudes with crudes of lower TAN, neutralizing the NAP or removing them from acidic crudes, using high quality alloys. Each of these methods can be expensive and increase production costs. The use of corrosion inhibitors is an attractive alternative to control NAP corrosion in refineries. A variety of different inhibitors have been developed, patented, and are currently in use for mitigating the NAP corrosion.[3-6] The chemical composition of commercial NAP corrosion inhibitors "currently in use" is proprietary, with patent literature revealing only that most are variations based on sulfur, phosphorous, or mixed P/S functional groups. Patents claim differences in delivery and structure of phosphorous or sulfur to form a "protective scale".

As users of such products, refineries are interested in lab tests that not only provide a relative measure of "efficiency" but also aid understanding of inhibitors reaction mechanism so that field application can be improved. Two phosphate ester corrosion inhibitors were experimentally evaluated as part of the Naphthenic Acid Corrosion Joint Industry Project (NAP JIP) at Ohio University. The performance and characteristics of the two corrosion inhibitors in two crude oil fractions are presented and discussed in the following sections.

EXPERIMENTAL

Experimental Procedure and Instrumentation

The corrosion inhibitors were evaluated according to a specific "pretreatment-challenge" corrosion test protocol.[8] It consists of two distinct phases and was designed to evaluate the properties of scales formed on metal surfaces from crude fractions at high temperature. Scales formed on test rings in autoclave at high temperature are characterized in the "pretreatment" phase. A second set of rings, pretreated in the same manner, are exposed during the "challenge" phase to high temperature, flow and shear stress conditions similar to those encountered in transfer lines of distilling units. The "challenge" phase is performed in a custom-designed "flow through" apparatus called the High Velocity Rig (HVR). The HVR flow path (Figure 1) includes an autoclave where the rings are rotated with 2000 rpm that corresponds to a peripheral velocity of 8.5 m/s. The HVR autoclave can be operated at pressures from 0 to 3.4 MPa (0 - 500 psig) and temperatures up to 370ºC (700ºF). The HVR metering pump provides a constant fluid flow of fresh feed in a range from 5 to 20 cm^3/min. All testing fluids and the HVR reactor are purged with nitrogen prior testing. The "pretreatment" phase is executed in a static autoclave -Figure 2 - (Parr Instruments Series 4520) that has a magnetic stirrer and can be operated to the same high temperature 370ºC (700ºF) as the HVR. Both experimental phases "pretreatment" and "challenge" had identical duration – 24h.

Based on their performance in previous corrosion tests, two crude fractions (VGO) were selected for evaluating inhibitors. The two VGO were provided by project sponsors along with their %S and TAN values. The two VGO were labeled as R (TAN = 0.78, S = 1.56 wt.%) and UB (TAN = 1.43, S = 2.89 wt.%). The inhibitors used in this experimental work were selected based on sponsors' requirements. Each inhibitor had to be of phosphate ester type and to be used in the industry at the date of the evaluation. The exact chemical structures and compositions of the two inhibitors were proprietary therefore they were labeled as inhibitor A and B.

Separate VGO only “pretreatment” tests were run as a reference for each “inhibitor & VGO” mixture. The inhibitor solutions for “pretreatment” phase were prepared by adding 500 ppm of inhibitor to 600 mL of VGO and then mixing the fluid thoroughly. For the “challenge” phase, a white mineral oil (no acid, no sulfur, no inhibitor) was spiked with commercial naphthenic acids (TCI America) to TAN = 3.5.

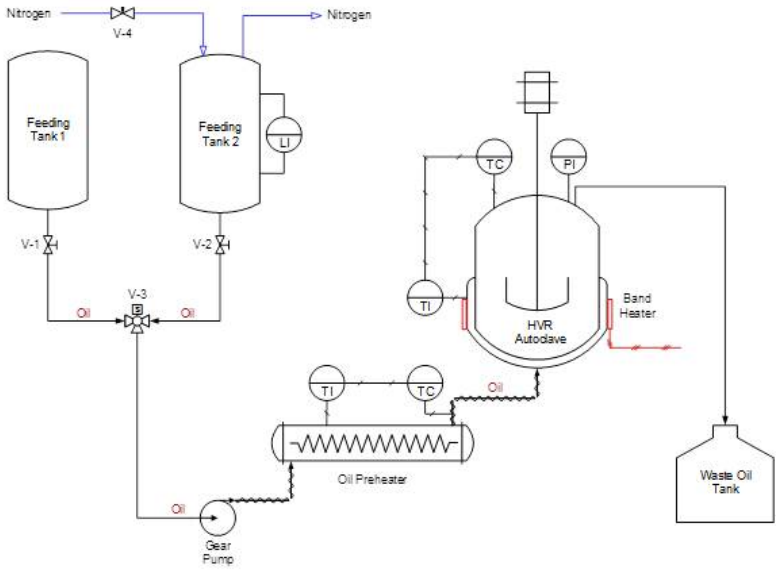

Figure 1: Schematic representation of the High Velocity Rig (HVR), the “flow through” loop used in “challenge” phase.

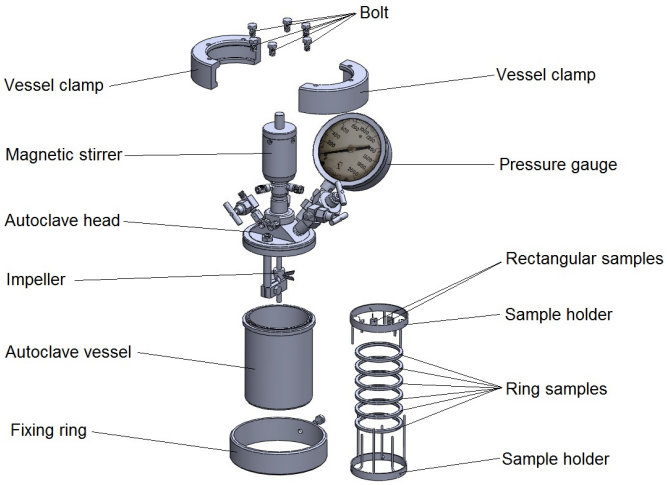

Figure 2: Static autoclave. Main components and samples set-up for the "pretreatment" experimental phase.

The sample rings with OD = 81.75 mm were made of UNS K03006 carbon steel (CS) and of UNS K41545 alloy steel (5Cr). Six rings were used in every experiment (3 of each type of steel).

Additional rectangular small samples made of same steel types were “pretreated” in autoclave tests and later used for SEM scale analysis. Corrosion rates were calculated based on samples metal losses. Before every test samples were polished with 400 and 600 grit silicon carbide (SiC) paper under isopropanol flush. Then samples were rinsed with acetone and dried under nitrogen flush. Samples were weighed on an analytical balance (initial weight) and their geometrical dimensions were measured with a caliper. When test ended the scales were removed from the samples by mechanical and chemical means. The superficial loose scale layers were removed by brushing the samples with a stiff plastic brush. Further, the strongly adherent scale persisting on the samples after mechanical brushing was chemically removed by using the Clarke solution (ASTM G 1-90).[9] At the end of the Clarke solution procedure the samples final weight was recorded and used in corrosion rate calculation.

Metal loss and scale gains were evaluated in every pre-treatment tests and these values were subtracted from samples initial weights that were exposed to a complete “pretreatment-challenge” test. By subtracting the metal losses corresponding to the “pretreatment” test, it became possible to quantify and evaluate precisely the corrosive effect of the NAP during the “challenge” phase.

Experimental conditions for corrosion inhibitor evaluation are summarized in Table 1.

Table 1
Experimental conditions for “pretreatment-challenge” tests with corrosion inhibitors.

Test Phase	**TAN** (mg KOH / g oil)	**Sulfur content** (wt %)	**Inhibitor conc.** (ppm)	**Temp.**	**Time** (h)	**Pressure** (psig)	**Rotation** (rpm)
“Pretreatment”	0.78 – 1.43	1.56 – 2.89	500	343ºC (650ºF)	24	200	0
“Challenge”	3.5	0	0	343ºC (650ºF)	24	150	2000

Cross sections of metal samples with scale intact were examined and analyzed using a JEOL JSM-6390 scanning electron microscope (SEM) coupled with an energy dispersive X-ray spectrometer (EDS). Thin cross sections of were ion milled and extracted from surfaces for examination by transmittance electron microscope (TEM) with Zeiss Libra 200EF (200 kV) also equipped with an energy dispersive X-ray spectrometer (EDS).

Experimental Data Processing

Corrosion rates expressed in *mm/y* were evaluated based on samples metal loss which were calculated as the difference between samples weight before and after the test, according to Equation 1.

$$CR = \frac{(IW - FW)}{\rho_{Fe} \cdot A_s \cdot t} \cdot 24 \cdot 365 \cdot 1000 \quad (1)$$

where

CR - corrosion rate [mm/y]
IW – initial weight [kg]
FW – final weight (after last clarking) [kg]

ρ_{Fe} – Steel density [kg/m^3]
A_s – sample area exposed to corrosive fluids [m^2]
t – time of the experiment [h]

As it was mentioned above separate "pretreatment" reference tests was performed and samples metal loss was evaluated in these tests. The “pretreatment” sample metal loss was then subtracted from the initial weight (IW) of every sample submitted to a complete "pretreatment-challenge" experiment. This “new” IW was then used in Equation 1 to calculate corrosion rates for the “challenge” phase. Thus, it was possible to separate the corrosive effects of “pretreatment” from those of the “challenge”.

Corrosion products build up on metal samples during the tests in form of scales. The analysis of these scales provides important information on the chemical reactions and their products formed during the runs. A theoretical scale thickness was calculated using Equation 2. It was assumed that scale formed uniformly on all samples surfaces and it consisted mainly of iron sulfide (FeS). The scale has a multilayered structure and during sample processing after the test, some of the superficial layers are lost in the solvent rinsing process. Therefore, in evaluation the scale thickness only the strongly adherent scale was considered. Thus, the weight gain is calculated as the difference between the sample weight after rubbing (mechanical removal) – W_{Rub} and the final weight of the samples after last clarking – FW.

$$\delta_A = \frac{(W_{Rub} - FW)}{\rho_{FeS} \cdot A_T} \cdot 10^6 \quad (2)$$

where

δ_A – adherent scale thickness [µm]
W_{Rub} – rub weight [kg]
FW – final weight (after last clarking) [kg]
ρ_{FeS} – iron sulfide density [kg/m^3]
A_T – sample total area exposed to corrosive fluids [m^2]

RESULTS AND DISCUSSION

Crude fractions corrosivity at high temperature is the result of combined effects of naphthenic acid and sulfur compounds which are part of the complex chemical composition of oils. The mechanism of naphthenic acids and sulfur corrosion is not fully deciphered yet but it is generally summarized by three chemical reactions.[9,10]

$$Fe + 2RCOOH \rightarrow Fe(RCOO)_2 + H_2 \quad (3)$$

$$Fe + H_2S \rightarrow FeS + H_2 \quad (4)$$

$$Fe(RCOO)_2 + H_2S \leftrightharpoons FeS + 2RCOOH \quad (5)$$

Main corrosion byproducts are iron naphthenates formed according to reaction (3) and iron sulfide (FeS) which is formed in reactions (4) and (5). Iron naphthenates are oil soluble and, in the absence of reactive sulfur, they can be entrained in the oil flow and constantly removed from the reaction sites. The iron sulfide is a solid corrosion product which is deposited in successive layers as it forms on the metal surfaces. However, imperfections in scale structure (cracks, pores) leave diffusion paths for NAP to partially dissolve the scale degrading its protective properties so that the underlying metal is attacked. According to reactions (4) and (5) and to experimental data the scale formed at high temperature from crude fractions consists mainly of FeS. However recently published studies revealed that NAP acid and sulfur corrosion is a more complicated process and scales formed in these reactions have a complex composition that also includes iron oxides (Fe_3O_4 magnetite) besides the FeS.[13-15] The complex structure of mixed scales has been used to rationalize and explain differences in corrosion resistance among scales.[12]

The scope of this work was to evaluate the efficiency of phosphate esters corrosion inhibitors in mitigating the NAP and S corrosion. The phosphate esters are proposed to interact with metal surfaces and inherent corrosion scale to form insoluble iron phosphate that covers these surfaces and protect them against the attack of corrosive species in oil.[15] The experimental results discussed in following paragraphs show the effect of the two phosphate esters in two high TAN VGO with different TAN/S content.

Corrosion Rate Results

Corrosion rates measured in experiments and calculated scale thicknesses for fraction R are plotted in Figure 3 &4 respectively. The corresponding results for fraction UB are given in Figures 5 &6.

Figure 3 compares the “pretreatment” and “challenge” corrosion rates of CS and 5Cr VGO R (TAN = 0.78., S = 1.56 wt.%) in the absence or in the presence of inhibitors. Without inhibitors – neat fraction R – the “challenge” corrosion rates were much higher than their corresponding “pretreatment” corrosion rates both for CS and 5Cr. The “challenge” rates for both metals were similar to those measured for specimens without pre-treatment, suggesting that scales formed in “pretreatment” with R provided limited protection against the NAP. Thickness calculations suggest that the NAP challenge had little effect on scale thickness (Figure 4)

Pretreatment of R containing 500 ppm inhibitor A showed reduced corrosion rates in “pretreatment”, especially for CS; corrosion rates in the corresponding “challenge” were much lower for both steel types. However, both CS and 5Cr “challenge” corrosion rates were higher than 1 mm/y indicating that inhibitor A had limited effect in R. Scale thickness did not appear to change significantly when A was added to fraction R.(Figure 4)

Inhibitor B had a major effect and significantly improved scale protective qualities when it was added to fraction R. Corrosion rates for CS and 5Cr, in “pretreatment” experiments with 500ppm inhibitor B were much lower than those for neat fraction R.(Figure 3). The scales formed when R was mixed with inhibitor B were very protective against the TAN 3.5 “challenge” with both CS and 5Cr corrosion rates close to 0. The very thin, highly protective scales were formed on CS and 5Cr samples in pretreatment with R containing inhibitor B (Figure 4). This suggests inhibitor B generates a scale that interferes with the formation of the thicker scale observed in the other fraction R tests.

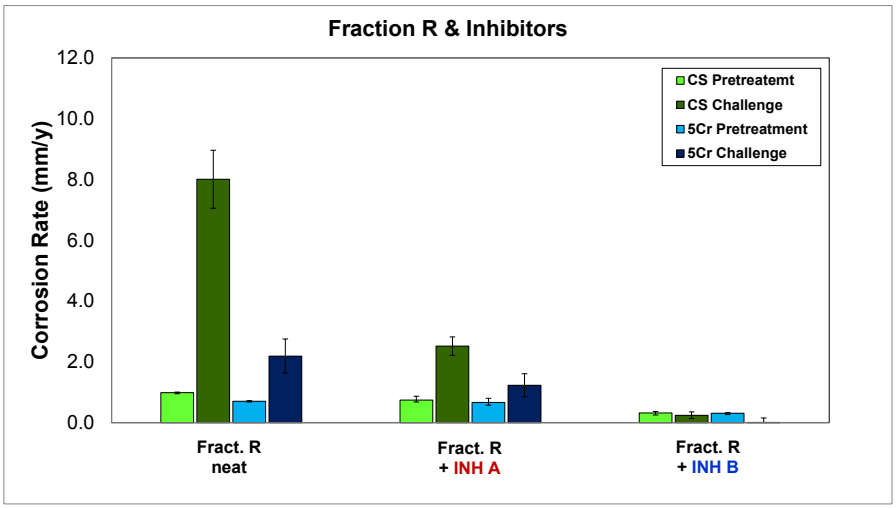

Figure 3: Corrosion rates of CS and 5Cr samples "pretreated" with fraction R neat, with R and inh. A and with R and inh. B, and then "challenged" with TAN 3.5 solution in the HVR.

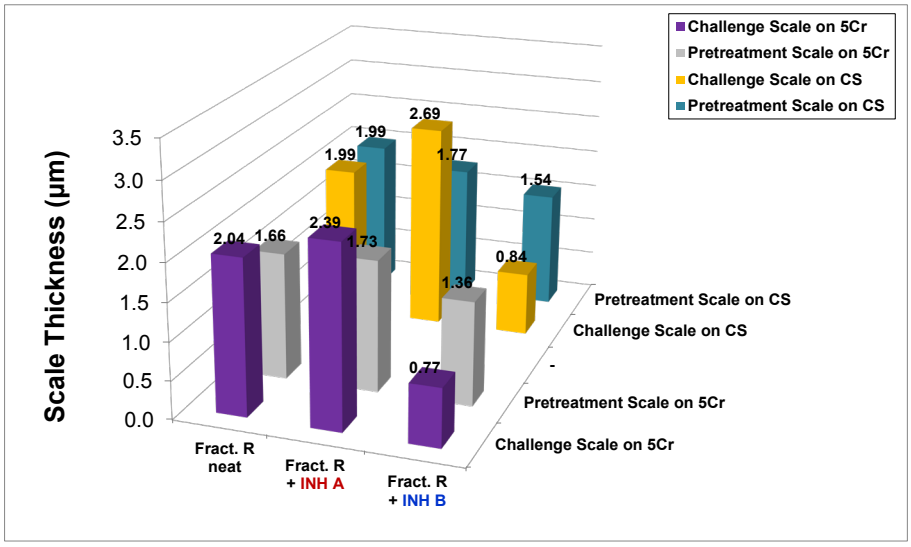

Figure 4: Comparison of scale thicknesses. Scales were formed on CS and 5Cr samples in autoclave "pretreatment" tests with fraction R neat, with R and inh. A, with R and inh. B and then the samples protected by scales were "challenged" with a TAN 3.5 solution in the HVR.

Duplicate "pretreatment-challenge" tests demonstrated high corrosion rates for neat Fraction UB with its high TAN and total S content (TAN = 1.43, S = 2.89 wt.%). The high "challenge" corrosion rates indicate that scales formed by neat UB on samples were not protective either metal (Figure 5).

Inhibitor A had a limited effect on fraction UB corrosivity in both stages of the test protocol. In comparison to neat UB, CS and 5Cr corrosion rates appear unaffected in by the addition of inhibitor B in "pretreatment" and were only slightly lower in the "challenge" (Figure 5). Likewise, similar scale thicknesses were detected in both stages for UB with or without inhibitor A. However, after "challenge" scales on both metals are much thinner than those after

"pretreatment" suggesting some partial scale removal under combination of NAP and shear stress (sample rotation) during the HVR "challenge".

On the other hand, Inhibitor B decreased fraction UB corrosivity in both stages and on both metals (Figure 5). The scales formed in UB and inhibitor B were thinner compared to those formed without inhibitor and their thickness did not change when "challenged" with NAP acids (Figure 6). The reduced corrosion rates and thickness of the scales appears to hint that inhibitor B generated a different type of scale that interfered with formation of the thicker scale inherent in the other UB tests.

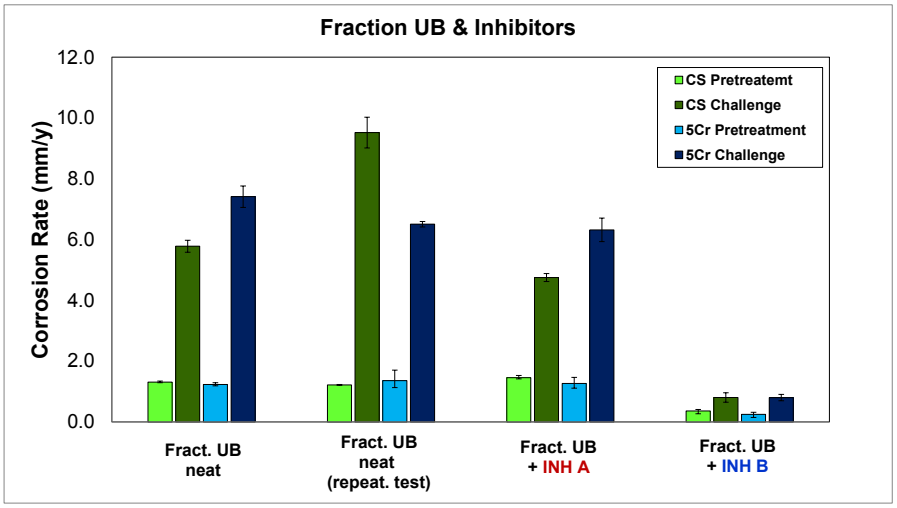

Figure 5: Corrosion rates of CS and 5Cr samples "pretreated" with fraction UB neat, with UB and inh. A and with UB and inh. B, and then "challenged" with TAN 3.5 solution in the HVR.

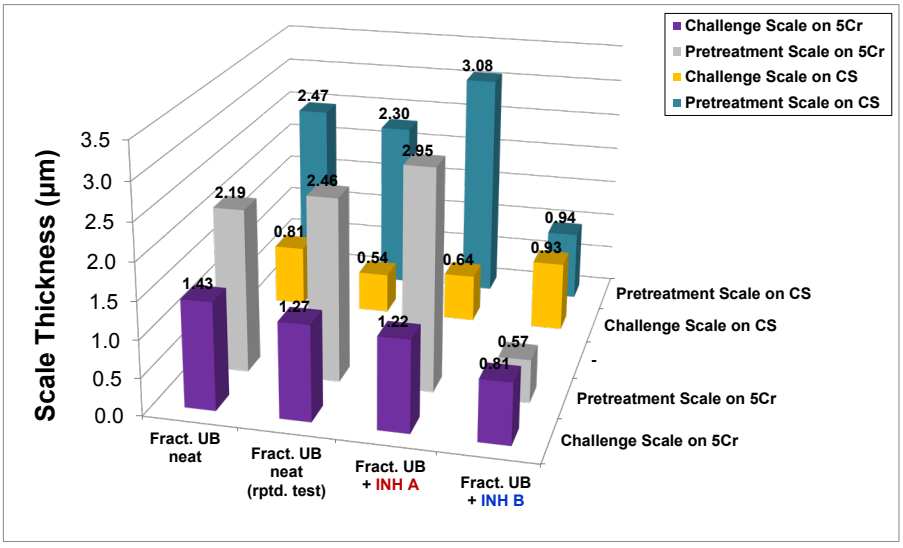

Figure 6: Comparison of scale thicknesses. Scales were formed on CS and 5Cr samples in autoclave "pretreatment" tests with fraction UB neat, with UB and inh. A, with UB and inh. B and then the samples protected by scales were "challenged" with a TAN 3.5 solution in the HVR.

Scales Analysis

Corrosion rate and scale thickness data does not explain the performance of inhibitors effect on crude fraction corrosivity. To gain some insight into the effects of the inhibitors on NAP corrosion, scales formed with R and UB mixed with inhibitors were analyzed in cross-section by SEM and TEM/EDS techniques. SEM images of scales formed with fraction R and inhibitors are compared on CS in Figure 7 and on 5Cr in Figure 8. In each figure, scales from "pretreatment" are shown above corresponding scale after NAP "challenge".

Neat fraction R forms a multilayered scale on CS in the autoclave "pretreatment" test (Figure 7(a). The fragmented structure of this scale facilitates the NAP acids diffusion that will corrode the metal and create large voids under scale during the "challenge" (Figure 7(d)). SEM images of scales formed from R mixed with inhibitor A and later "challenged" do not differ significantly from those formed without inhibitor (Figure 7(b) and (e)). The similarities between the two scale examples suggest the limited effect of inhibitor A on fraction R corrosivity, an observation supported by the corresponding corrosion rates measured in these tests.

Likewise, fraction R with or without inhibitor A forms non-protective, multilayered scales on 5Cr and these scales survive the TAN 3.5 "challenge" while corrosion proceeds. (Figure 8). However, fraction R with inhibitor B forms a thin film on 5Cr that protects very effectively against NAP attack on the base metal.

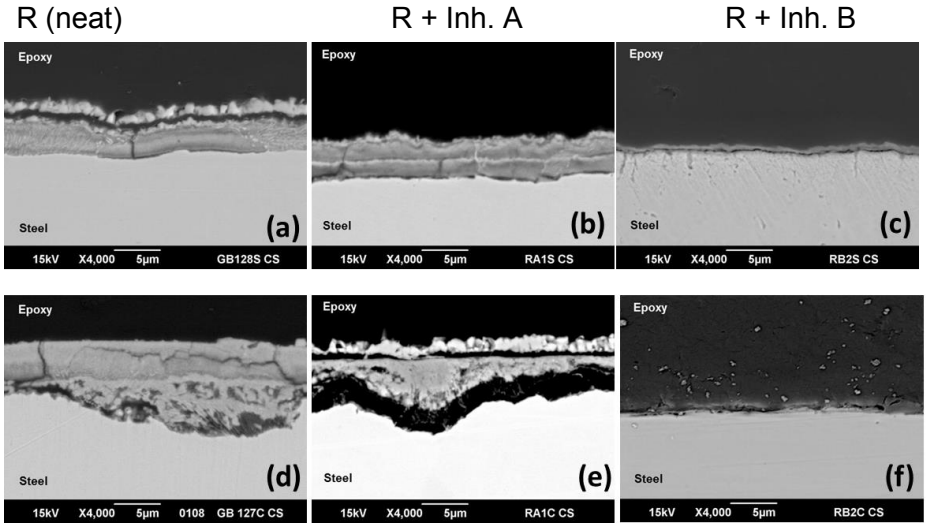

Figure 7: SEM cross-section images of scales formed on CS samples: (a) "pretreatment" scale formed with fraction R neat, (d) same scale after TAN 3.5 "challenge"; (b) "pretreatment" scale formed with fraction R + Inh. A, (e) same scale after TAN 3.5 "challenge"; (c) "pretreatment" scale formed with fraction R + Inh. B, (f) same scale after TAN 3.5 "challenge".

Similar SEM scale images were observed on both metals in tests on fraction UB; so only those for CS are shown (Figure 9). SEM images confirm that Fraction UB formed thicker scales than fraction R, most probably due to its higher total S content (2.89 wt.%). However, the scale thickness did not offer a better protection to the metal during the "challenge" phases. NAP acids diffused through the thick scale and corroded extensively the metal leaving large voids under

the scale. These voids are consistent with the reduction is scale “thickness” calculated by weight loss (Figure 6). Inhibitor A added to UB did not affect scale characteristics in either stage of the protocol (Figure 9 (b) & (e)). In contrast, inhibitor B added to fraction UB created a protective scale barely detectable in the SEM images (Figure 9 (c) & (f)).

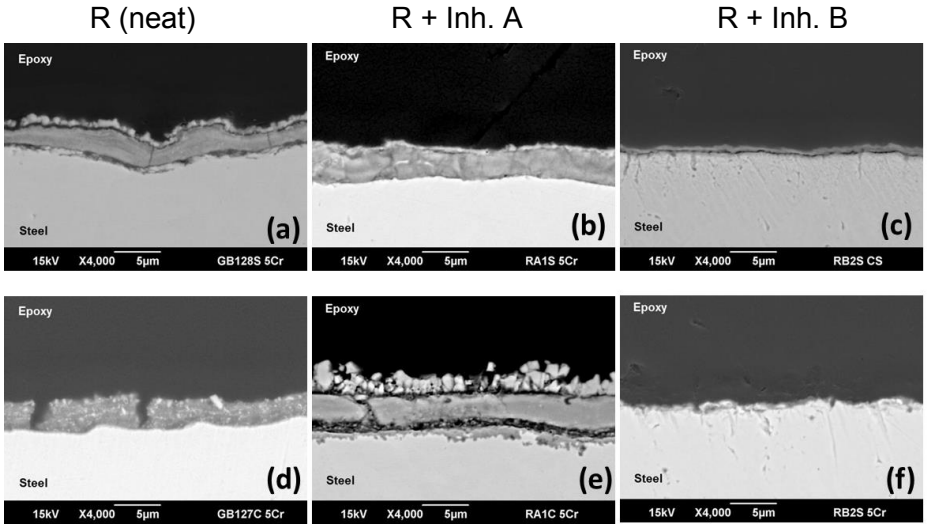

Figure 8: SEM cross-section images of scales formed on 5Cr samples: (a) “pretreatment” scale formed with fraction R neat, (d) same scale after TAN 3.5 “challenge”; (b) “pretreatment” scale formed with fraction R + Inh. A, (e) same scale after TAN 3.5 “challenge”; (c) “pretreatment” scale formed with fraction R + Inh. B, (f) same scale after TAN 3.5 “challenge”.

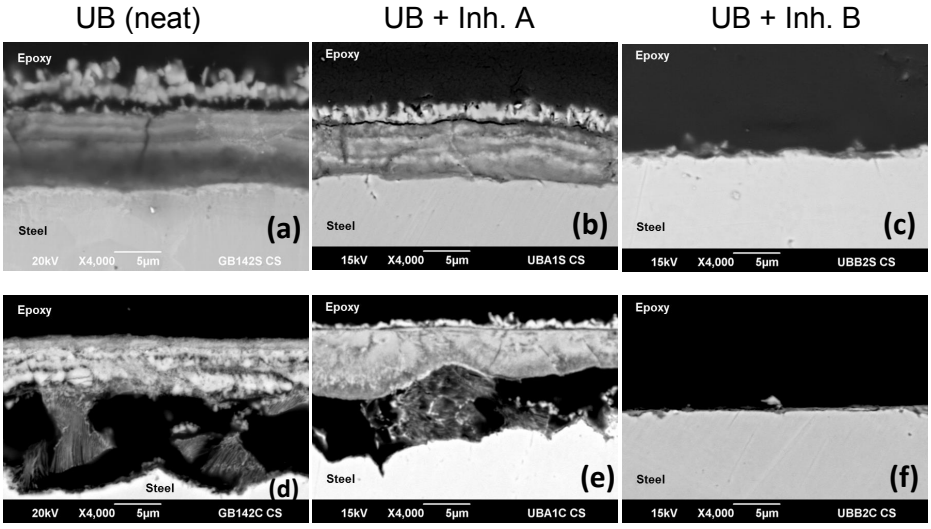

Figure 9: SEM cross-section images of scales formed on CS samples: (a) “pretreatment” scale formed with fraction UB neat, (d) same scale after TAN 3.5 “challenge”; (b) “pretreatment” scale formed with fraction UB + Inh. A, (e) same scale after TAN 3.5 “challenge”; (c) “pretreatment” scale formed with fraction UB + Inh. B, (f) same scale after TAN 3.5 “challenge”.

Scale TEM Analysis

Inhibitor B formed protective scales both with fractions R and B that were too thin to properly characterize by SEM (Figures 7-9). Therefore, representative CS samples were selected for analysis of the scales by TEM/EDS which has higher resolution that allowed elemental mapping and EDS analysis (atomic %) on selected points (Figures 10-13).

CS samples pretreated with inhibitor A in R and UB are compared in Figures 10 & 11. Elemental mapping for CS "pretreated" in R with inhibitor A (Figure 10 (a)) shows that the scale was rich in sulfur (yellow) and iron (red) with smaller amounts of oxygen (blue). Phosphorus (magenta) appears to be only on top of the scale which suggests that the inhibitor was not able to reach the metal and form the iron phosphate. EDS point analysis confirms that scale formed in R containing inhibitor A consisted mainly of FeS (Figure 10 b and Table 2).

TEM/EDS analyses for CS samples "pretreated" with fraction UB containing inhibitor A were similar to those in fraction R. Elemental mapping analysis of scale on CS indicates that it consists mainly of FeS without incorporation of phosphorous from the inhibitor (Figure 11 (a)). . EDS point analysis measures S, Fe and P in the scale but it also detects significant amounts of oxygen which might be present in form of iron oxide (Table 3).

Two CS samples exposed to Inhibitor B were analyzed by TEM/EDS: one was after "pretreatment" in fraction R; the other after pretreatment in fraction R and NAP 3.5 challenge. Corrosion rates measured on CS in these experiments were very low suggesting the existence of a very protective scale/film that was barely visible in the SEM cross-section images of these samples. The TEM/EDS offered a more complete view of these scales. Specifically, the EDS elemental mapping shows a multilayered scale with an intermediate layer rich in phosphorus and oxygen (Figure 12 (a)). Underneath this thin, homogeneous layer there is another layer rich in oxygen an iron (probably an iron oxide). A thick layer consisting only of sulfur and iron is covering the thinner inner layers. The EDS point analysis shows in that the intermediate homogenous thin layer consists mainly of phosphorus, oxygen, and iron (Table 4 – point 2) and it is probably iron phosphate. Further, the results of Table 4 indicate that layer located under the intermediate one contains mainly oxygen and iron with some traces of sulfur (point 1) and top thick later is mainly FeS (point 3 & 4). Phosphorus and oxygen were also detected in on the top of the FeS thick layer (point 5).

The TEM image reveals a very thin layer (~ 200 nm) with a relatively homogeneous structure after "challenge" of a scale formed with R containing inhibitor B (Figure 13 (b)). The thin scale is made of phosphorus (magenta), oxygen (yellow) and iron (red) according to elemental mapping data (Figure 13 (a)). The EDS elemental mapping of this layer indicate phosphorus (magenta), oxygen (yellow) and iron (red) as the main component of it (Figure 13 (a)). The mapping results corroborated by elemental point analysis (Table 4). The latter hints that the TAN 3.5 challenge strips FeS from the scale leaving a surviving scale rich in iron phosphate.

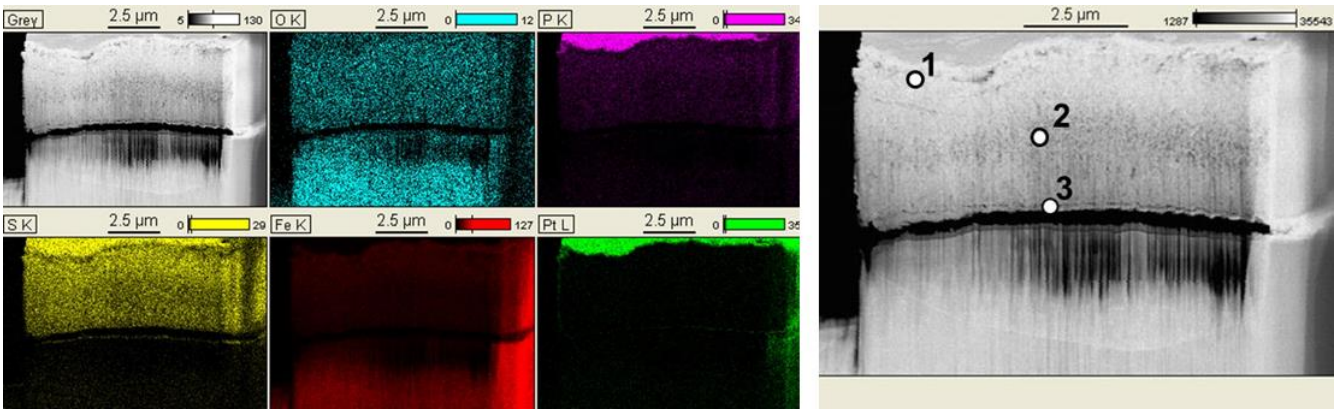

(a) (b)

Figure 10: TEM/EDS analysis of a scale formed on CS in "pretreatment" with fraction R and inhibitor A – (a) scale elemental mapping and (b) selected points on the scale for EDS elemental analysis. Point analysis results presented in Table 2.

Table 2
EDS point analysis results for scale formed on CS sample in "pretreatment" with fraction R and inhibitor A

Point	1	2	3
Element Line	Atom %	Atom %	Atom %
O-K	7.4	13.4	14
P-K	4.3	0	0
S-K	45.3	48.2	41
Fe-K	43	38.3	45
Total	100	100	100

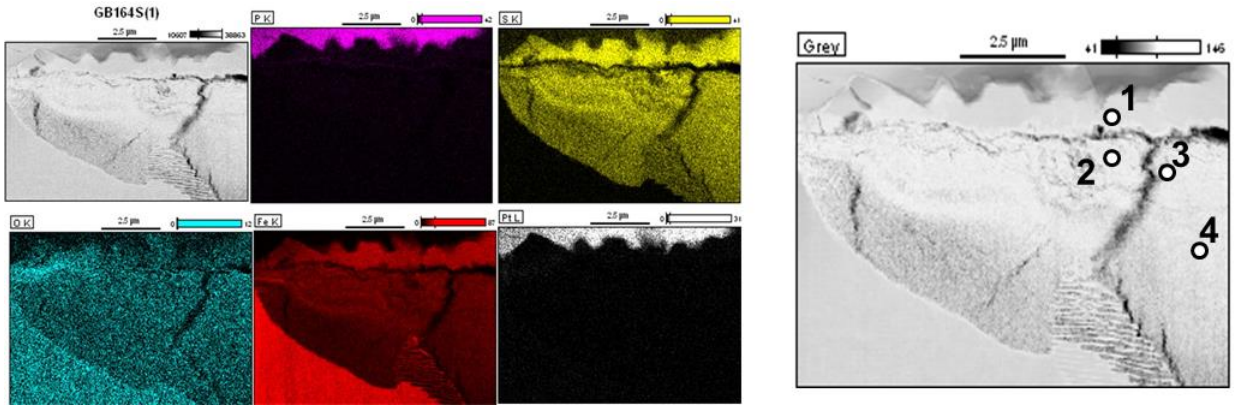

(a) (b)

Figure 11: TEM/EDS analysis of a scale formed on CS in "pretreatment" with fraction UB and inhibitor A – (a) scale elemental mapping and (b) selected points on the scale for EDS elemental analysis. Point analysis results are summarized in Table 3.

Table 3
EDS point analysis results for scale formed on CS sample in "pretreatment" with fraction UB and inhibitor A

Point	1	2	3	4
Element Line	Atom %	Atom %	Atom %	Atom %
O-K	0.3	26.7	10.7	11.3
P-K	5.3	7.2	0	0
S-K	3.2	29.4	48.3	31.6
Fe-K	6.9	36.6	41	57.1
Pt-K	84.3	0.1	0.1	0.1
Total	100	100	100	100

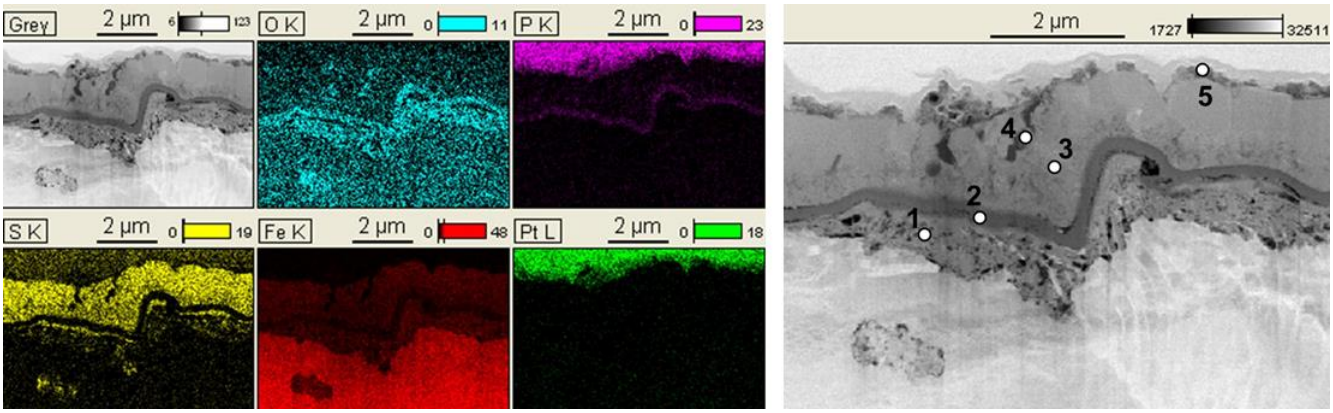

(a) (b)

Figure 12: TEM/EDS analysis of a scale formed on CS in "pretreatment" with fraction R and inhibitor B – (a) scale elemental mapping and (b) selected points on the scale for EDS elemental analysis. Point analysis results are summarized in Table 4.

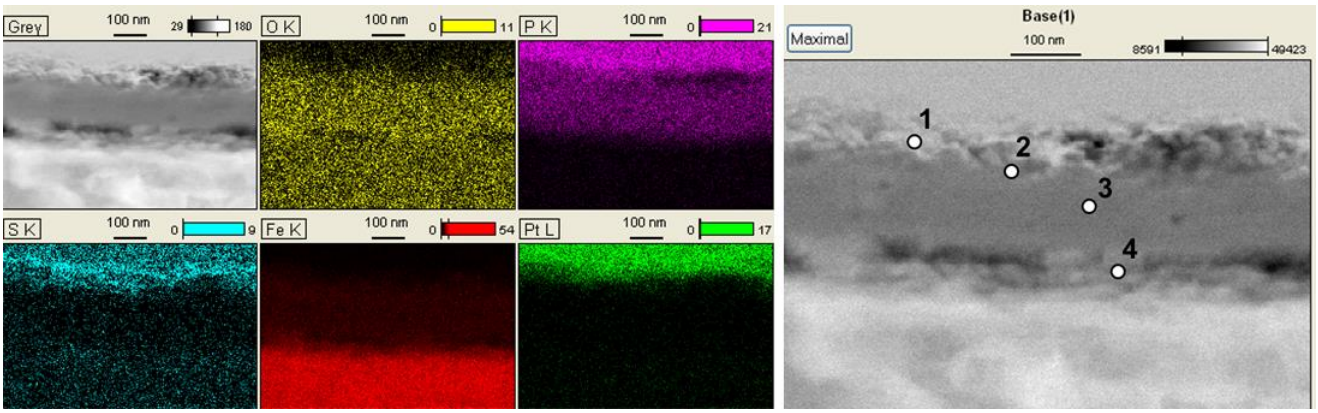

(a) (b)

Figure 13: TEM/EDS analysis of a scale formed on CS in "pretreatment" with fraction R and inhibitor A and then "challenged" with NAP acid (TAN 3.5) – (a) scale elemental mapping and (b) selected points on the scale for EDS elemental analysis. EDS point analysis results are summarized in Table 5.

Table 4
EDS point analysis results for scale formed in "pretreatment" with fraction R and inhibitor B and later "challenged" with NAP acid (TAN 3.5)

	Pretreatment (Figure 12 - b)					Pretreatment-Challenge (Figure 13 - b)			
Point	1	2	3	4	5	1	2	3	4
Element Line	Atom %	Atom %	Atom %	Atom %	Atom %	Atom %	Atom %	Atom %	Atom %
O-K	53.3	62.7	24.6	59.8	30	37.4	39.9	41.1	30.3
P-K	0.3	10.7	3.4	5.3	42.4	25	30.2	32.6	11.9
S-K	14.7	7	39.6	18.5	5.1	3.8	0	0	0.1
Fe-K	31.7	19.6	32.5	16.4	22.6	24.6	29.9	26.2	57.6
Pt-K	0	0	0	0	0	9.1	0	0.1	0.1
Total	100	100	100	100	100	100	100	100	100

CONCLUSIONS

The influence of two phosphate NAP corrosion inhibitors (A&B) on CS and 5Cr has been evaluated using a "pretreatment-challenge" testing protocol that determines corrosion rates and characterizes surface scale. Each inhibitor was tested in two crude oil fractions (R & UB) and results compared for inhibitor-free fractions for stage of the test protocol.

Inhibitor A slightly improved protectiveness in "R" scales but had no influence on scale protectiveness in "UB" which had ~ 2x higher TAN & S content. On the other hand, Inhibitor B was very effective in providing protectiveness for both crude fractions. Cross-section TEM/EDS data showed that Inhibitor A had little or no effect on the structure or composition micron thick scales in either crude fraction with little phosphorous detected suggesting that the inhibitor did not compete with the reactive S and NAP that formed the S- & O- rich scale. In the "challenge" stage, inhibitor A scales were undermined in the same way as the inhibitor-free scales which explains the lack of corrosion resistance..

In contrast, tests with Inhibitor B in either crude fraction left thin (sub-micron) scales layer visible only in the TEM images. TEM/EDS analysis a distribution of S, O & P throughout the scale formed in "pretreatment" that appears depleted in S after the TAN 3.5 challenge. These observations suggest that Inhibitor B competes with the indigenous reactive S and NAP to form a protective iron phosphate phase in the thin scale. The "challenge" did not appear to affect the iron phosphate.

The TEM/EDS data suggest that the difference in efficiency between these two commercial phosphate ester corrosion inhibitors can be explained by differences in their competition with native corrosive species in oil (NAP acids and S). These differences may be attributed to differences in phosphate ester structure and composition that deliver phosphorous to the surface.

AKNOWLEDGEMENTS

The authors are grateful to all companies that supported financially the NAP JIP research project at Ohio University and allowed them to publish the results of this experimental work. The authors would also like to thank the staff from Swagelok Center for Center Analysis of Materials at Case Western Reserve University for all their help and assistance with the TEM/EDS analysis.

REFERENCES

1. Gutzeit, J.; Naphthenic Acid Corrosion in Oil Refineries. *Mater. Perform*. **1977**, *16*, 24-35.
2. Piehl, R.L.; Naphthenic Acid Corrosion in Crude Distillation Units. *Mater. Perform.* **1988**, *27* (1), 37-43.
3. Petersen, P.R.; Robbins, III, F.P.; Winston, W.G. Naphthenic Acid Corrosion Inhibitors, U.S. Patent 5,182,013, Jan. 26, **1993**.
4. Edmondson, J.G. High Temperature Corrosion Inhibitor, U.S. Patent 5,500,107, Mar. 19, **1996**.
5. Babaian-Kibala, E.; Hyatt, J.G.; Rose, T.J.; Use of Sulfiding Agents for Enhancing the Efficacy of Phosphorous in Controlling High Temperature Corrosion Attack, U.S. Patent 5,630,964, May 20, **1997**.
6. Zetlmeisl, M. J. Control of Naphthenic Acid Corrosion with Thiophosphorous Compounds, U.S. Patent 5,863,415, Jan. 26, **1999**.
7. Georgescu, O.; Constantinescu, G, Ilie, M; Georgescu, A.D.; Anticor Type Romanian Made Corrosion Inhibitors for Refineries and Petrochemical Plant Equipment. *Mater. Corros.* **2000**, *51*, 152-154.
8. Wolf, H.A.; Cao, F.; Blum, S.C.; Schilowitz, A.M.; Ling, S.; McLaughlin, J.E.; Nesic, S.; Jin, P.; Bota, G.; Method for Identifying Layers Providing Corrosion Protection in Crude Oil Fractions. U.S. Patent 9,140,640 B2, Sep. 22, 2015.
9. ASTM G 1-90 (2011) “Standard Practice for Preparing, Cleaning, and Evaluating Corrosion Test Specimens”.(West Conshohocken, PA, Annual Book of ASTM Standards, ASTM).
10. Slavcheva, E.; Shone, B. Turnbull, A.; Review of Naphthenic Acid Corrosion in Oil Refining. **1999**. *Br.Corros. J.* 34, (2), 125-131.
11. Yépez, O.; Influence of Different Sulfur Compunds on Corrosion Due Naphthenic Acid. *Fuel*. **2005**. *84*, 97-104.
12. Jin, P.; Robbins, W.; Bota, G. Mechanism of magnetite formation in high temperature corrosion by model naphthenic acids. *Corros. Sci.* **2016**. *111*, 822–834.
13. Jin, P.; Bota, G.; Robbins, W.; Nesic, S.; Analysis of oxide scales formed in the naphthenic acid corrosion of carbon steel, *Energy Fuels*, **2016**. *30*, 6853-6862.
14. Barney, M.M.; Embaid, B.P.; Nissan, A.; Indentifying phases in protective scale formed during high temperature. *Corros. Sci.* **2017**. *127*, 21-26.
15. Babaian-Kibala, E.; Phosphate Ester Inhibitors Solve Naphthenic Acid Corrosion Problems *Oil Gas J.* **1994**. *92*(9), 31-35.